RSC Advances

PAPER

View Article Online
View Journal | View Issue

Open Access Article. Published on 14 2017. Downloaded on 25/08/2025 10:45:53.
This article is licensed under a Creative Commons Attribution 3.0 Unported Licence.

Check for updates

Cite this: RSC Adv., 2017, 7, 52694

Value of *mir-247* in warning of graphene oxide toxicity in nematode *Caenorhabditis elegans*†

Guosheng Xiao,[a] Lingtong Zhi,[b] Xuecheng Ding,[c] Qi Rui[c] and Dayong Wang *[ab]

Received 17th August 2017
Accepted 3rd November 2017

DOI: 10.1039/c7ra09100a

rsc.li/rsc-advances

Graphene oxide (GO) induces some dysregulated microRNAs (miRNAs), such as *mir-247*, in *Caenorhabditis elegans*. We here further investigated the role and value of *mir-247* in detecting GO toxicity in nematodes after prolonged exposure. In nematodes, *mir-247* acted in neurons to regulate GO toxicity, and neuronal overexpression of *mir-247* induced a susceptibility to GO toxicity. We detected the significant increase in *mir-247* in wild-type nematodes exposed to GO at concentrations of more than 10 μg L^{-1}. Moreover, we found the GO toxicity in a transgenic strain overexpressing neuronal *mir-247* after exposure to GO at concentrations of more than 10 μg L^{-1}. Therefore, our results imply the important potential of *mir-247* in warning of the formation of GO toxicity in the range of μg L^{-1} in nematodes.

Introduction

Graphenic nanomaterials, such as graphene oxide (GO), are one of the most fascinating nanostructures with unique physical and chemical properties, and are potentially used in biosensors, bio-imaging, cancer therapy, and drug delivery.[1–3] Meanwhile, both *in vitro* and *in vivo* studies have suggested the potential pulmonary toxicity, reproductive toxicity, and toxic effect on immune response of GO in human cell lines or mammals.[4–7] *Caenorhabditis elegans*, a classic model animal, can offer an *in vivo* assay system for elucidating the toxicological mechanisms of toxicants, including engineered nanomaterials.[8] In nematodes, it was reported that GO exposure could cause toxic effects on the functions of both primary (such as intestine) and secondary (such as neuron and reproductive organs) targeted organs.[9–12]

For the cellular mechanism of GO toxicity in nematodes, it has been shown that activation of oxidative stress, bioavailability, intestinal permeability, defecation behavior, and innate immune response may contribute greatly to the formation of GO toxicity.[9,10,13] For the underlying molecular mechanisms of GO toxicity in nematodes, insulin, p38 mitogen-activated protein kinase (MAPK), cell death and DNA damage, and oxidative stress or response associated signaling pathways have been shown to be involved in the control of GO toxicity.[12,14–16] Moreover, the potential toxic effects from GO exposure can be inhibited by the treatment with glycyrrhizic acid, an active component from *Glycyrrhizae radix*, or lactic acid bacteria.[11,17]

The short noncoding microRNAs (miRNAs) have been shown to exist in many organisms, including *C. elegans*.[18] miRNAs usually act to suppress the expression of certain targeted genes post-transcriptionally.[19] So far, the dysregulated miRNAs have already been identified in GO exposed nematodes, and the potential function of some dysregulated miRNAs have been further confirmed using the corresponding mutants.[20] Among these candidate miRNAs, our previous study has suggested that GO exposure could increase the expression of *mir-247*.[20] Meanwhile, the *mir-247/797* mutant showed the resistant property to GO toxicity on lifespan and aging related phenotypes,[20] implying that the activated *mir-247* may mediate the molecular mechanism for the GO toxicity formation. However, the environmental implication of *mir-247* in the safety assessment of GO exposure is still unclear. Thus, we here further employed *in vivo* assay system of *C. elegans* to investigate the potential value of *mir-247* expression in the safety assessment of environmental GO exposure. In *C. elegans*, *mir-247* is expressed in several tissues, including pharynx and neurons.[21,22] We also examined the tissue-specific activity of *mir-247* in affecting the induction of GO toxicity. Our results suggest the potential value of alteration in *mir-247* expression in the assessment or prediction of toxicity induced by environmental exposure to GO.

Experimental

Preparation and characterization of GO

GO was prepared from natural graphite powder using the modified Hummer's method.[23] Graphite (2 g) and sodium nitrate (1 g) were added into a 250 mL flask. Concentrated H_2SO_4 (50 mL) was added on ice, and $KMnO_4$ (7 g) was further added. After the mixture temperature reached to 35 °C, H_2O

[a]College of Biology and Food Engineering, Chongqing Three Gorges University, Wanzhou 404100, China. E-mail: dayongw@seu.edu.cn

[b]Key Laboratory of Environmental Medicine Engineering in Ministry of Education, Medical School, Southeast University, Nanjing 210009, China

[c]College of Life Sciences, Nanjing Agricultural University, Nanjing 210095, China

† Electronic supplementary information (ESI) available. See DOI: 10.1039/c7ra09100a

This journal is © The Royal Society of Chemistry 2017

Open Access Article. Published on 14 2017. Downloaded on 25/08/2025 10:45:53.
This article is licensed under a Creative Commons Attribution 3.0 Unported Licence.

(90 mL) was slowly dripped into the paste to dilute it. After stirring the diluted suspension at 70 °C for 15 min, the suspension was treated with a mixture of 7 mL of 30% H_2O_2 and 55 mL of H_2O. The resulting warm suspension was filtered to obtain a yellow-brown filter cake, which was washed with 3% HCl, followed by drying at 40 °C for 24 h. GO would be obtained after ultrasonication of as-made graphite oxide in water for 1 h.

GO was characterized by atomic force microscopy (AFM, SPM-9600, Shimadzu, Japan), Raman spectroscopy using a 632 nm wavelength excitation (Renishaw Invia Plus laser Raman spectrometer, Renishaw, UK), and zeta potential determined by dynamic light scattering (DLS) using a Nano Zetasizer (Malvern Instrument Ltd., UK). Based on the AFM assay, the thickness of GO was approximately 1.0 nm in topographic height, corresponding to the property of one layer (Fig. 1a). Sizes of GO in K-medium after sonication (40 kHz, 100 W, 30 min) were mainly in the range of 40–50 nm (Fig. 1b). Raman spectroscopy assay indicated the existence of G band at 1592 cm^{-1} and D band at 1326 cm^{-1} (Fig. 1c). The zeta potential of GO (10 mg L^{-1}) in K-medium was −22.3 ± 2.7 mV.

C. elegans strains and exposure

Nematodes used were wild-type N2, mutant of *mir-247/797(n4505)*, and transgenic strains of *mir-247/797(n4505) Ex(Pmir-247-mir-247)*, *mir-247/797(n4505)Ex(Pmir-797-mir-797)*, *mir-247/797(n4505)Ex(Punc-14-mir-247)*, *mir-247/797(n4505) Ex(Pmyo-2-mir-247)*, and *Ex(Punc-14-mir-247).* Some of the used strains were from *Caenorhabditis* Genetics Center (funded by NIH Office of Research Infrastructure Programs (P40 OD010440)). Nematodes were maintained on nematode growth medium (NGM) plates seeded with *Escherichia coli* OP50 at 20 °C as described.[24] The nematodes were lysed with a bleaching mixture (0.45 mol L^{-1} NaOH, 2% HOCl) after washing off the plates into centrifuge tubes, and age synchronous L1-larvae populations were prepared as described.[25]

Exposure and toxicity assessment

After sonication for 30 min (40 kHz, 100 W), GO was dispersed in K medium to prepare the stock solution (1 mg mL^{-1}). GO at working concentrations were prepared by diluting the stock solution with K medium. Prolonged exposure to GO was performed from L1-larvae to adult day-1 (approximately 4.5 days) in liquid K medium in 12-well sterile tissue culture plates at 20 °C in the presence of food (OP50). After prolonged exposure to GO, the examined nematodes were used for toxicity assessment using lifespan and intestinal reactive oxygen species (ROS) production as the endpoints.

Lifespan assay was preformed at 20 °C basically as described.[26,27] During the lifespan assay, hermaphrodite nematodes were transferred daily for the first 7 days of adulthood. Nematodes were checked every day, and scored as dead if they did not move even after repeated taps with a pick. Sixty nematodes were examined per treatment, and three replicates were performed.

Intestinal ROS production assay was performed as described previously.[28,29] The endpoint of intestinal ROS production was used to reflect the induction of oxidative stress. After prolonged exposure to GO, the examined nematodes were transferred to 1 μmol L^{-1} 5′,6′-chloromethyl-2′,7′-dichlorodihydro-fluorescein diacetate (CM-H2DCFDA; Molecular Probes) to incubate for 3 h in the dark. The nematodes were examined under a laser

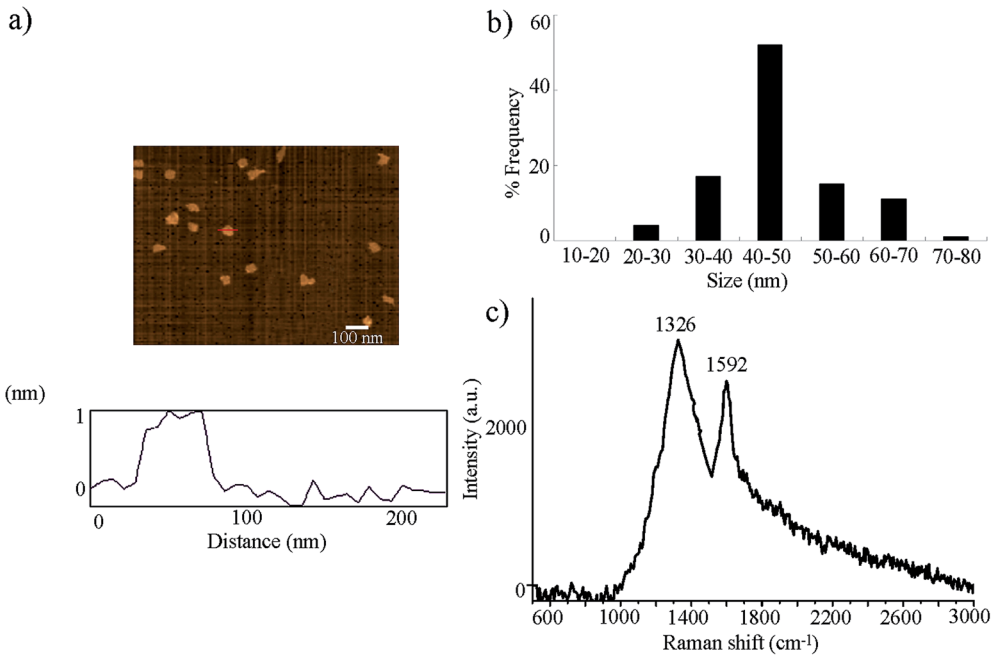

Fig. 1 Physiochemical properties of GO. (a) AFM analysis of GO after sonication. (b) Size distribution of GO after sonication. (c) Raman spectrum of GO.

Open Access Article. Published on 14 2017. Downloaded on 25/08/2025 10:45:53.
This article is licensed under a Creative Commons Attribution 3.0 Unported Licence.

scanning confocal microscope (Leica, TCS SP2, Bensheim, Germany) at 488 nm of excitation wavelength and at 510 nm of emission filter. Relative fluorescence intensity of ROS signals in intestine was semi-quantified, and expressed as relative fluorescence units (RFU). Sixty nematodes were examined per treatment.

Reverse-transcription and quantitative real-time polymerase chain reaction (PCR)

Total RNA was isolated from the nematodes using Trizol reagent (Invitrogen, UK) according to manufacturer's protocol. The extracted RNA was used for the further cDNA synthesis. Relative expression levels of the *mir-247* were measured by real-time PCR (RT-PCR) in an ABI 7500 with Evagreen (Biotium, USA). Three biological replicates were performed. Expression of *mir-247* or *mir-797* is presented as relative expression ratio between *mir-247* or *mir-797* and *F35C11.9*, which encodes a small nuclear RNA U6. The related primer information is shown in Table S1.†

DNA constructs and germline transformation

To generate entry vector carrying promoter sequence, promoter region for *unc-14* gene specially expressed in neurons, *myo-2* gene specially expressed in pharynx, *mir-247*, or *mir-797* was amplified by PCR from wild-type *C. elegans* genomic DNA. These promoter fragments were inserted into pPD95_77 vector in the sense orientation. *mir-247* or *mir-797* was amplified by PCR, and inserted into corresponding entry vector carrying the *unc-14*, *myo-2*, *mir-247*, or *mir-797* promoter sequence. Transformation was performed by coinjection testing DNA at the concentration of 10–40 μg mL^{-1} and marker DNA of P*dop-1::rfp* at the concentration of 60 μg mL^{-1} into the gonad of nematodes as described.[30] The related primer information for DNA constructs is shown in Table S2.†

Statistical analysis

Data in this article were expressed as means ± standard deviation (SD). Statistical analysis was performed using SPSS 12.0 software (SPSS Inc., Chicago, USA). Differences between groups were determined using analysis of variance (ANOVA), and probability levels of 0.05 and 0.01 were considered statistically significant. The lifespan data were analyzed using a 2-tailed 2 sample *t*-test (Minitab Ltd, Coventry, UK).

Results

Confirmation of the contribution of *mir-247* in the regulation of GO toxicity

mir-247/797(n4505) mutant contains both the mutation of *mir-247* and the mutation of *mir-797*, and was resistant to GO toxicity in reducing lifespan and in inducing ROS production (Fig. 2).[20] To determine whether the resistance of *mir-247/797(n4505)* mutant to GO toxicity is due to the functional deficit in *mir-247*, *mir-247* or *mir-797* was expressed in *mir-247/797(n4505)* mutant. The expression of *mir-247* or *mir-797* in *mir-247/797(n4505)* mutant was confirmed by qRT-PCR (Fig. S1†). It was reported that prolonged exposure (from L1-larvae to young adults) to GO at the concentrations more than 1000 μg L^{-1} could decrease the locomotion behavior and induce the significant induction of intestinal ROS production in nematodes.[9] We selected 10 000 μg L^{-1} as the working concentration for GO to confirm the contribution of *mir-247* in the regulation of GO toxicity. After GO exposure, expression of *mir-797* did not significantly affect the lifespan and the induction of ROS production in *mir-247/797(n4505)* mutant (Fig. 2). In contrast, after GO exposure, expression of *mir-247* significantly suppressed the resistance of *mir-247/797(n4505)* mutant to GO toxicity in reducing lifespan and in inducing ROS production, and the phenotypes of lifespan and induction of ROS production in GO exposed *mir-247/797(n4505)Ex(Pmir-247-mir-247)* were similar to those in GO exposed wild-type nematodes (Fig. 2). Therefore, the formation of resistance in *mir-247/797(n4505)* mutant to GO toxicity may be due to the mutation of *mir-247*.

Tissue-specific activity of *mir-247* in the regulation of GO toxicity

Using tissue-specific promoters, we further examined the tissue-specific activity of *mir-247* in the regulation of GO toxicity. Expression of *mir-247* in neurons or pharynx in *mir-247/797(n4505)* mutant was confirmed by qRT-PCR (Fig. S2†). Rescue assay by expression of *mir-247* in the pharynx did not significantly affect the resistance of *mir-247/797(n4505)* mutant to GO (10 000 μg L^{-1}) toxicity in reducing lifespan and in inducing ROS production (Fig. 3). In contrast, expression of *mir-247* in the neurons significantly inhibited the resistance of *mir-247/797(n4505)* mutant to GO (10 000 μg L^{-1}) toxicity in reducing lifespan and in inducing ROS production (Fig. 3). Therefore, *mir-247* may act in the neurons to regulate the GO toxicity.

Neuronal overexpression of *mir-247* enhanced the GO toxicity

To further investigate the function of neuronal *mir-247* in the regulation of GO toxicity, we generated the transgenic strain overexpressing neuronal *mir-247*. Overexpression of *mir-247* in *Ex(Punc-14-mir-247)* was confirmed by qRT-PCR (Fig. S3†). Under normal conditions, the transgenic strain of *Ex(Punc-14-mir-247)* exhibits the similar lifespan to wild-type nematodes, and do not show the obvious induction of ROS production (Fig. 4). However, after GO (10 000 μg L^{-1}) exposure, the transgenic strain of *Ex(Punc-14-mir-247)* showed the more decreased lifespan and the more severe induction of ROS production than those in wild-type nematodes (Fig. 4). Therefore, overexpression of neuronal *mir-247* may induce the enhancement of GO toxicity in nematodes.

Toxicity assessment of GO in nematodes overexpressing neuronal *mir-247*

We next performed the toxicity assessment of GO at different concentrations in nematodes overexpressing neuronal *mir-247* using intestinal ROS production as the endpoint. After

Open Access Article. Published on 14 2017. Downloaded on 25/08/2025 10:45:53.
This article is licensed under a Creative Commons Attribution 3.0 Unported Licence.

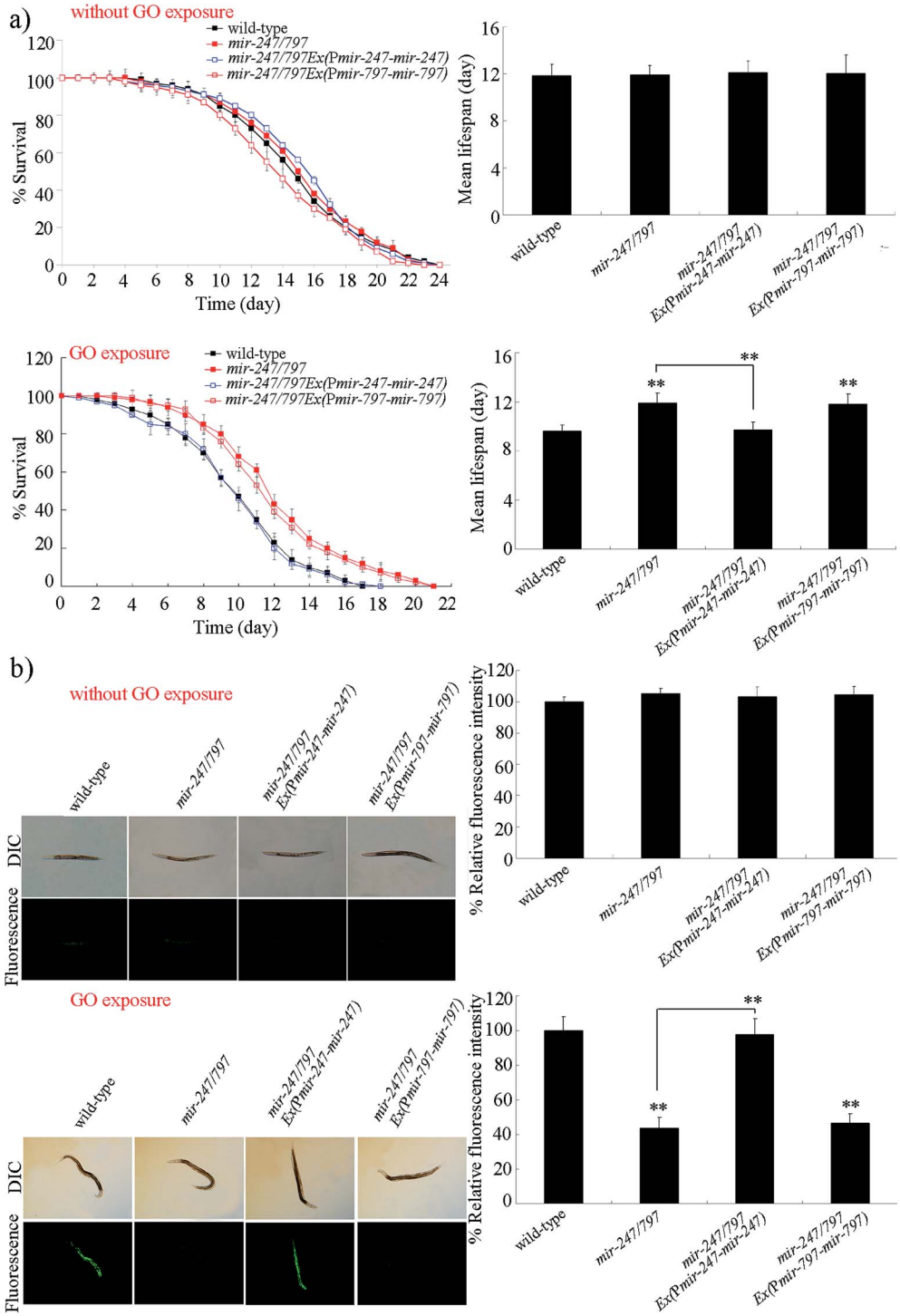

Fig. 2 Rescue assay of GO toxicity in *mir-247/797* mutant nematodes. (a) Rescue assay of GO toxicity on lifespan in *mir-247/797* mutant nematodes. (b) Rescue assay of GO toxicity in inducing intestinal ROS production in *mir-247/797* mutant nematodes. GO exposure concentration was 10 000 μg L^{-1}. Prolonged exposure was performed from L1-larvae to adult day-1. Bars represent means ± SD. $^{**}P < 0.01$ *vs.* wild-type (if not specially indicated).

prolonged exposure, we observed that GO at concentrations more than 100 μg L^{-1} caused the significant induction of intestinal ROS production in wild-type nematodes (Fig. 5). In contrast, we detected the significant induction of intestinal ROS production in nematodes overexpressing neuronal *mir-247* exposed to GO at concentrations more than 10 μg L^{-1} (Fig. 5). Moreover, the induction of intestinal ROS production was more severe in nematodes overexpressing neuronal *mir-247* than that in wild-type nematodes after exposure to GO at the concentration of 100 or 1000 μg L^{-1} (Fig. 5).

Open Access Article. Published on 14 2017. Downloaded on 25/08/2025 10:45:53.
This article is licensed under a Creative Commons Attribution 3.0 Unported Licence.

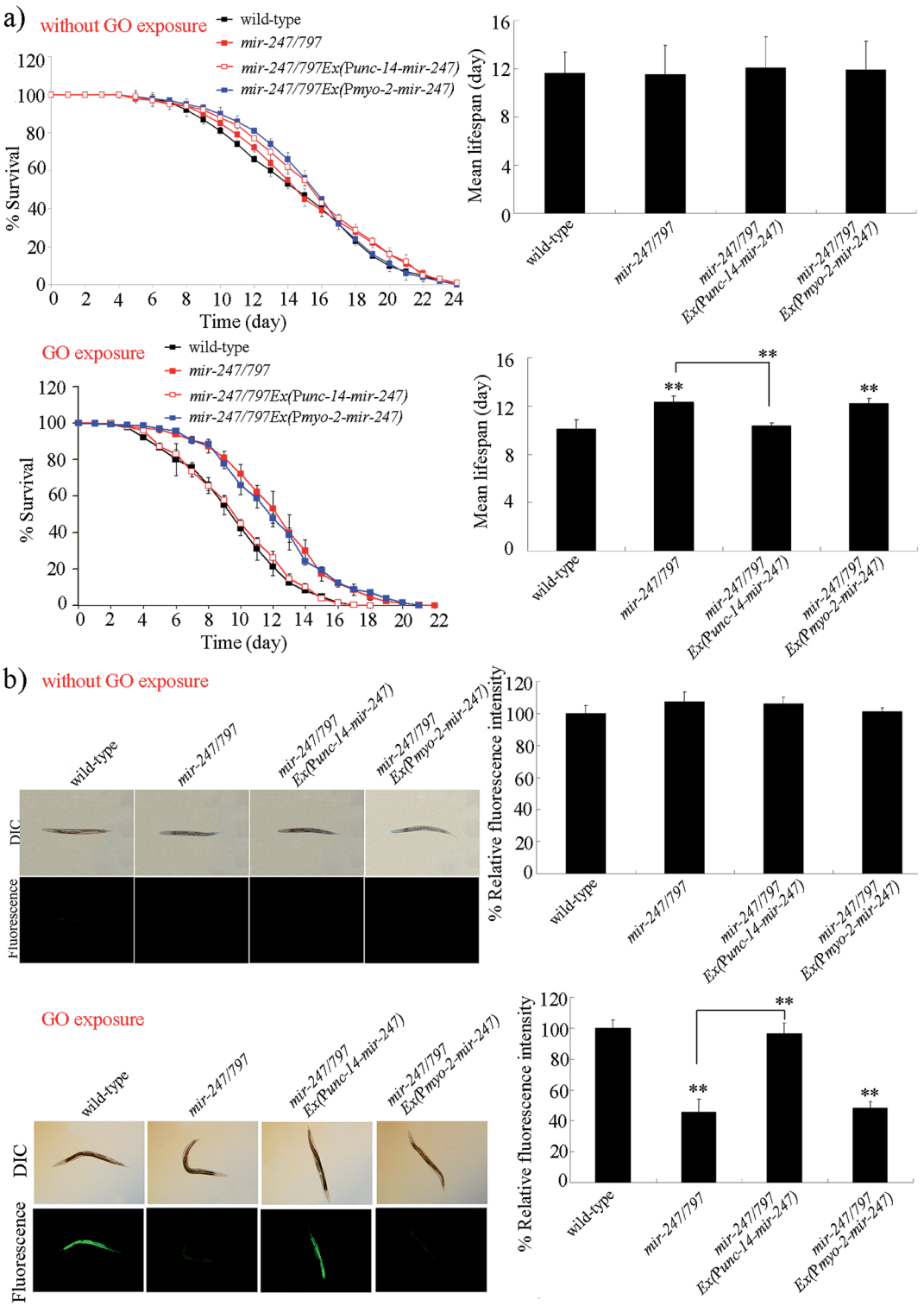

Fig. 3 Tissue-specific activity of *mir-247* in the regulation of GO toxicity. (a) Tissue-specific activity of *mir-247* in the regulation of GO toxicity on lifespan. (b) Tissue-specific activity of *mir-247* in the regulation of GO toxicity in inducing intestinal ROS production. GO exposure concentration was 10 000 μg L^{-1}. Prolonged exposure was performed from L1-larvae to adult day-1. Bars represent means ± SD. $^{**}P < 0.01$ *vs.* wild-type (if not specially indicated).

Alteration in *mir-247* expression in GO exposed wild-type nematodes

We further investigated the expressional alteration of *mir-247* in GO exposed wild-type nematodes. After prolonged exposure to 1 μg L^{-1} of GO, we did not detect the obvious alteration in *mir-247* expression (Fig. 6). However, we observed the significant increase in *mir-247* expression in wild-type exposed to GO at concentrations more than 10 μg L^{-1} (Fig. 6).

 This journal is © The Royal Society of Chemistry 2017

Open Access Article. Published on 14 2017. Downloaded on 25/08/2025 10:45:53.
This article is licensed under a Creative Commons Attribution 3.0 Unported Licence.

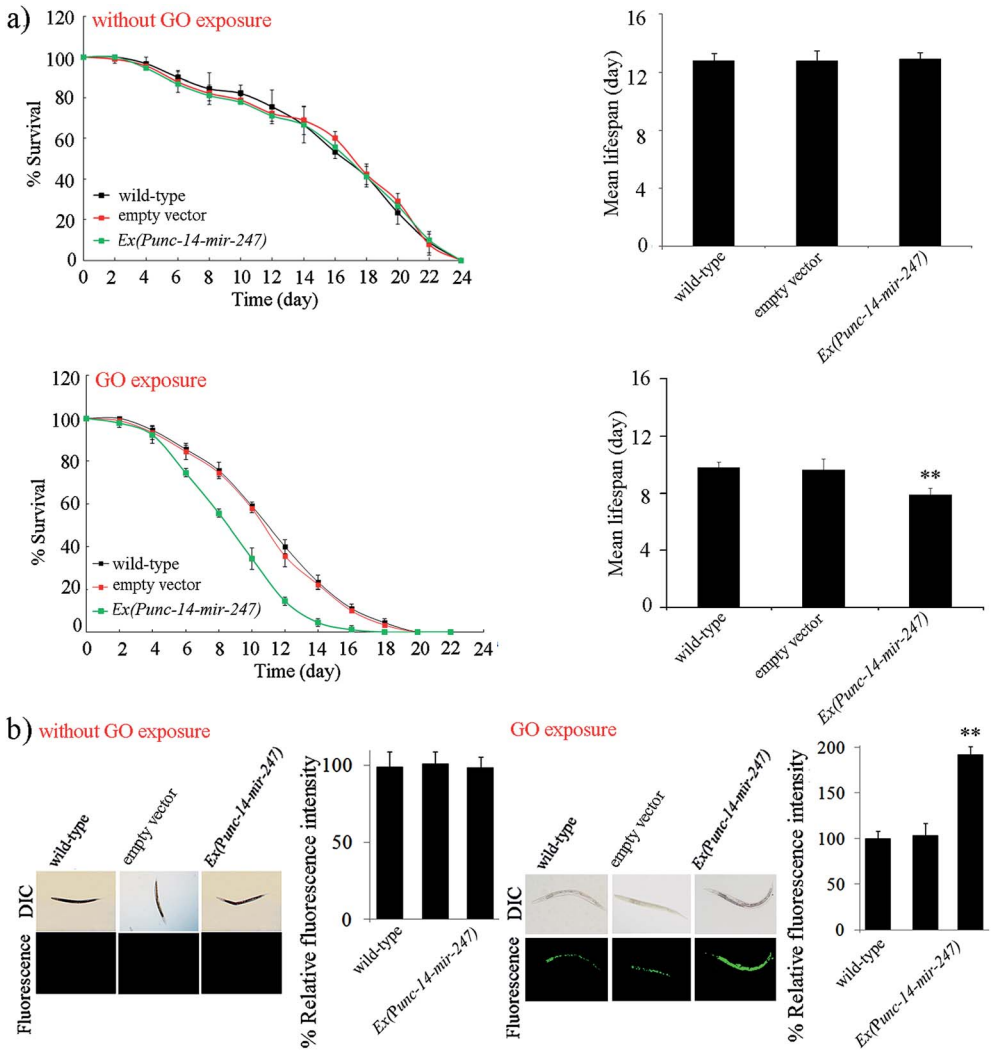

Fig. 4 Effect of neuronal overexpression of *mir-247* on GO toxicity. (a) Effect of neuronal overexpression of *mir-247* on GO toxicity in reducing lifespan. (b) Effect of neuronal overexpression of *mir-247* on GO toxicity in inducing intestinal ROS production. GO exposure concentration was 10 000 μg L^{-1}. Prolonged exposure was performed from L1-larvae to adult day-1. Bars represent means ± SD. $^{**}P < 0.01$ *vs.* wild-type.

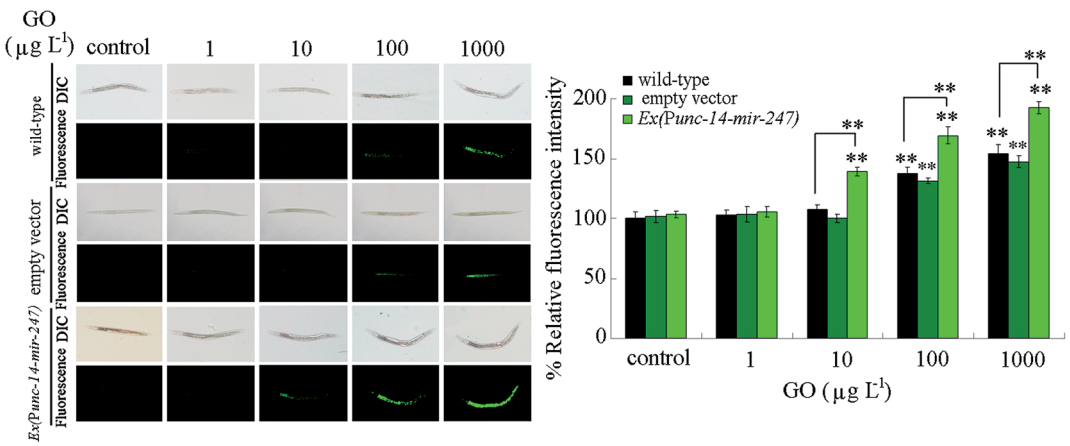

Fig. 5 Toxicity assessment of GO in nematodes overexpressing neuronal *mir-247* using intestinal ROS production as the endpoint. Prolonged exposure was performed from L1-larvae to adult day-1. Bars represent means ± SD. $^{**}P < 0.01$ *vs.* control (if not specially indicated).

Open Access Article. Published on 14 2017. Downloaded on 25/08/2025 10:45:53.
This article is licensed under a Creative Commons Attribution 3.0 Unported Licence.

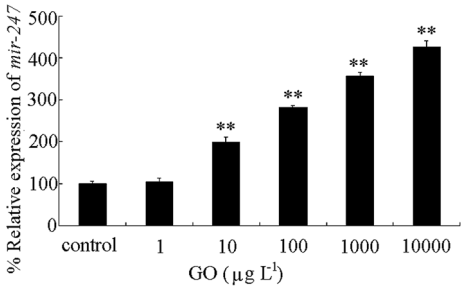

Fig. 6 Expression of *mir-247* in wild-type nematodes after prolonged exposure. Prolonged exposure was performed from L1-larvae to adult day-1. Bars represent means ± SD. $^{**}P < 0.01$ *vs.* control.

Discussion

It has been shown that *mir-247* is involved in the control of male tail development, and overexpression of *mir-247* induces the abnormalities in mail tail rays.[22] In this study, we provide the direct evidence to indicate the involvement of *mir-247* in the control of GO toxicity. The rescue assays demonstrated that that the observed resistance of *mir-247/797(n4505)* mutant to GO toxicity in reducing lifespan and in inducing ROS production was due to the mutation of *mir-247* (Fig. 2). In addition, GO exposure could increase the transcriptional expression of *mir-247* in nematodes.[20] These results suggest that *mir-247* may positively regulate the toxicity formation of certain environmental toxicants, such as GO. Under normal conditions, mutation or overexpression of *mir-247* did not induce the significant intestinal ROS production (Fig. 2b and 4b). Therefore, although *mir-247* may not regulate the oxidative stress under normal conditions, overexpression of *mir-247* may induce a susceptibility to oxidative stress or stress response in nematodes. In nematodes, PEG surface modification or fetal bovine serum (FBS) coating could reduce GO toxicity.[31] Meanwhile, we observed that PEG surface modification or FBS coating could further suppress the *mir-247* expression in GO exposed nematodes (Fig. S4†), which further confirms the potential role of *mir-247* in the regulation of GO toxicity. Nevertheless, we did not observe the significant alteration in *mir-247* expression in reduced graphene oxide (rGO) or multiwalled carbon nanotubes exposed nematodes (data not shown).[32]

In *C. elegans*, insulin and p38 mitogen-activated protein kinase (MAPK) signaling pathways have been shown to act in the intestine to regulate the GO toxicity.[15,33,34] Moreover, cell apoptosis and DNA damage signaling pathways may function in the germline to regulate the reproductive toxicity of GO.[16] In this study, *mir-247* may mediate a certain molecular signaling in the neurons to regulate the GO toxicity, since *mir-247* expression in the neurons suppressed the resistance of *mir-247/797(n4505)* mutant to GO toxicity (Fig. 3). Therefore, so far, at least the intestine, the neurons, and the germline, as well as the molecular signals in these organs, may participate in the control of GO toxicity in nematodes. More recently, the ERK signaling was also identified to act in the neurons to regulate the GO toxicity, and the increased expression of neuronal ERK signaling may mediate a protection mechanism for nematodes against the GO toxicity.[35] In nematodes, GO is mainly distributed in intestine, pharynx, and reproductive organs, such as gonad.[36]

In this study, we further provide evidence to indicate that neuronal overexpression of *mir-247* induced a susceptibility to GO toxicity (Fig. 4). Using the transgenic strain overexpressing neuronal *mir-247* could even detect the toxicity of GO at the concentration of 10 μg L^{-1} (Fig. 5). It is normally predicted that the environmentally relevant concentrations of engineered nanomaterials (ENMs) are in the range of ng L^{-1} or μg $^{L-1}$.[37,38] It was reported that certain genetic mutants can be employed to detect the toxicity of ENMs at environmentally relevant concentrations in nematodes.[39] Our results suggest that, besides certain genetic mutants, certain transgenic strains could also be helpful for detecting the possible toxicity of ENMs at environmentally relevant concentrations.

In wild-type nematodes, we further found that prolonged exposure to GO at concentrations more than 10 μg L^{-1} could significantly increase the *mir-247* expression (Fig. 6). Meanwhile, we only detected the toxicity in wild-type nematodes exposed to GO at concentrations more than 100 μg L^{-1} (Fig. 5). These observations imply that the increase in *mir-247* may provide a potential warning for the formation of GO toxicity in 10 μg L^{-1} of GO exposed nematodes.

In nematodes, using TargetScan version 6.2 (http://www.targetscan.org/worm_52/), a large amount of genes may act as the targets of *mir-247* (Table S3†). In the list of potential targeted genes for *mir-247*, we did not find the genes required for the control of oxidative stress. We detected some genes encoding components in important signaling pathways in this list. For example, *cwn-1* encodes a Wnt ligand in the Wnt signaling pathway, *pkc-1* encodes a serine/threonine protein kinase in the ERK signaling pathway, and *goa-1* encodes a heterotrimeric G protein in the G-protein signaling pathway. It has been reported that at least CWN-1 and PKC-1 are involved in the control of GO toxicity in nematodes.[29,40]

Conclusions

In this study, we determined the role and value of *mir-247* in the detection of GO toxicity using *in vivo* assay system of *C. elegans*. In nematodes, *mir-247* acted in the neurons to regulate GO toxicity. Neuronal overexpression of *mir-247* induced a susceptibility to GO toxicity. In wild-type nematodes, we detected the toxicity of GO at concentrations more than 100 μg L^{-1}. In contrast, we could observe the toxicity in nematodes exposed to GO at concentrations more than 10 μg L^{-1} in transgenic strain overexpressing neuronal *mir-247*. More importantly, we found the significant increase in *mir-247* in nematodes exposed to GO at concentrations more than 10 μg L^{-1}. Our results suggest the important value of increase in *mir-247* in warning the potential of GO toxicity in nematodes.

Conflicts of interest

There are no conflicts to declare.

 This journal is © The Royal Society of Chemistry 2017

Open Access Article. Published on 14 2017. Downloaded on 25/08/2025 10:45:53.
This article is licensed under a Creative Commons Attribution 3.0 Unported Licence.

References

1 A. K. Geim, *Science*, 2009, **324**, 1530–1534.
2 D. Bitounis, H. Ali-Boucetta, B. H. Hong, D. Min and K. Kostarelos, *Adv. Mater.*, 2013, **25**, 2258–2268.
3 K. Yang, S. Zhang, G. Zhang, X. Sun, S. Lee and Z. Liu, *Nano Lett.*, 2010, **10**, 3318–3323.
4 K. Yang, Y. Li, X. Tan, R. Peng and Z. Liu, *Small*, 2013, **9**, 1492–1503.
5 G. Qu, S. Zhang, L. Wang, X. Wang, B. Sun, N. Yin, X. Gao, T. Xia, J. Chen and G. Jiang, *ACS Nano*, 2013, **7**, 5732–5745.
6 Y. P. Li, Q. L. Wu, Y. L. Zhao, Y. F. Bai, P. S. Chen, T. Xia and D. Y. Wang, *ACS Nano*, 2014, **8**, 2100–2110.
7 S. Liang, S. Xu, D. Zhang, J. He and M. Chu, *Biomaterials*, 2015, **9**, 92–105.
8 Y. L. Zhao, Q. L. Wu, Y. P. Li and D. Y. Wang, *RSC Adv.*, 2013, **3**, 5741–5757.
9 Q. L. Wu, L. Yin, X. Li, M. Tang, T. Zhang and D. Y. Wang, *Nanoscale*, 2013, **5**, 9934–9943.
10 Q. L. Wu, Y. L. Zhao, J. P. Fang and D. Y. Wang, *Nanoscale*, 2014, **6**, 5894–5906.
11 Y. L. Zhao, X. M. Yu, R. H. Jia, R. L. Yang, Q. Rui and D. Y. Wang, *Sci. Rep.*, 2015, **5**, 17233.
12 Y. L. Zhao, Q. L. Wu and D. Y. Wang, *RSC Adv.*, 2015, **5**, 92394–92405.
13 W. Zhang, C. Wang, Z. Li, Z. Lu, Y. Li, J. Yin, Y. Zhou, X. Gao, Y. Fang, G. Nie and Y. Zhao, *Adv. Mater.*, 2012, **24**, 5391–5397.
14 Q. L. Wu, Y. L. Zhao, Y. P. Li and D. Y. Wang, *Nanoscale*, 2014, **6**, 11204–11212.
15 Y. L. Zhao, R. L. Yang, Q. Rui and D. Y. Wang, *Sci. Rep.*, 2016, **6**, 24024.
16 Y. L. Zhao, Q. L. Wu and D. Y. Wang, *Biomaterials*, 2016, **79**, 15–24.
17 Y. L. Zhao, R. H. Jia, Y. Qiao and D. Y. Wang, *Nanomedicine*, 2016, **12**, 735–744.
18 V. Ambros, R. C. Lee, A. Lavanway, P. T. Williams and D. Jewell, *Curr. Biol.*, 2003, **13**, 807–818.
19 D. P. Bartel, *Cell*, 2004, **116**, 281–297.
20 Q. L. Wu, Y. L. Zhao, G. Zhao and D. Y. Wang, *Nanomedicine*, 2014, **10**, 1401–1410.
21 N. J. Martinez, M. C. Ow, J. S. Reece-Hoyes, M. I. Barrasa, V. R. Ambros and A. J. Walhout, *Genome Res.*, 2008, **18**, 2005–2015.
22 H. Zhang and S. W. Emmons, *Dev. Dyn.*, 2009, **238**, 595–603.
23 N. I. Kovtyukhova, P. J. Olivier, B. R. Martin, T. E. Mallouk, S. A. Chizhik, E. V. Buzaneva and A. D. Gorchinskiy, *Chem. Mater.*, 1999, **11**, 771–778.
24 S. Brenner, *Genetics*, 1974, **77**, 71–94.
25 S. Donkin and P. L. Williams, *Environ. Toxicol. Chem.*, 1995, **14**, 2139–2147.
26 S. Shakoor, L. M. Sun and D. Y. Wang, *Toxicol. Res.*, 2016, **5**, 492–499.
27 J. N. Yang, Y. L. Zhao, Y. W. Wang, H. F. Wang and D. Y. Wang, *Toxicol. Res.*, 2015, **4**, 1498–1510.
28 Q. L. Wu, P. D. Liu, Y. X. Li, M. Du, X. J. Xing and D. Y. Wang, *J. Environ. Sci.*, 2012, **24**, 733–742.
29 H. Chen, H. R. Li and D. Y. Wang, *Sci. Rep.*, 2017, **7**, 41655.
30 C. Mello and A. Fire, *Methods Cell Biol.*, 1995, **48**, 451–482.
31 Q. L. Wu, X. F. Zhou, X. X. Han, Y. Z. Zhuo, S. T. Zhu, Y. L. Zhao and D. Y. Wang, *Biomaterials*, 2016, **102**, 277–291.
32 Y. L. Zhao, Q. L. Wu, Y.-P. Li, A. Nouara, R. H. Jia and D. Y. Wang, *Nanoscale*, 2014, **6**, 4275–4284.
33 Y. L. Zhao, L. T. Zhi, Q. L. Wu, Y. L. Yu, Q. Q. Sun and D. Y. Wang, *Nanotoxicology*, 2016, **10**, 1469–1479.
34 M. X. Ren, L. Zhao, X. Lv and D. Y. Wang, *Nanotoxicology*, 2017, **11**, 578–590.
35 M. Qu, Y. H. Li, Q. L. Wu, Y. K. Xia and D. Y. Wang, *Nanotoxicology*, 2017, **11**, 520–533.
36 Q. L. Wu, Y. L. Zhao, J. P. Fang and D. Y. Wang, *Nanoscale*, 2014, **6**, 5894–5906.
37 F. Gottschalk, T. Sonderer, R. W. Scholz and B. Nowack, *Environ. Sci. Technol.*, 2009, **43**, 9216–9222.
38 N. Mueller and B. Nowack, *Environ. Sci. Technol.*, 2008, **42**, 4447–4453.
39 Q.-L. Wu, Y.-L. Zhao, Y.-P. Li and D.-Y. Wang, *Nanomedicine*, 2014, **10**, 1263–1271.
40 L. T. Zhi, M.-X. Ren, M. Qu, H. Y. Zhang and D. Y. Wang, *Sci. Rep.*, 2016, **6**, 39261.